ANALYSIS OF CANTING STRATEGIES USING THE HFLCAL MODEL

Willem Landman[1], and Paul Gauché[2]

[1] Solar Thermal Energy Research Group, Stellenbosch University, Knowledge Centre, Corner of Banghoek and Joubert Street, Stellenbosch, South Africa; Phone: +27 (0) 84 400 2014; E-mail: wlandman@sun.ac.za

[2] Solar Thermal Energy Research Group, Stellenbosch University, E-mail: paulgauche@sun.ac.za

Abstract

The Levelised Cost of Energy of a central receiver system can be reduced if improvements in the optical performance of a heliostat outweigh the $/m^2 cost. Selecting an optimum heliostat canting strategy leads to an improvement in heliostat performance. The choice of canting strategy is thought to have minor cost implications, since heliostat facets require precision alignment regardless of the canting strategy chosen. The HFLCAL model is adapted to incorporate canting strategies, allowing an analytical calculation of the performance. Results of on-axis and off-axis canting are compared to a reference case and correlate to within 5 %. Performance trends are found to be consistent and it is concluded that the model is appropriate for preliminary analysis of canting strategies, thus providing a computationally inexpensive analytical tool.

Keywords: heliostat; optics; canting strategy.

1. Introduction

The Levelised Cost of Energy (LCOE) of concentrating solar power (CSP) must be significantly reduced to compete with fossil fuel technologies. In a central receiver system (CRS) the heliostat field contributes approximately 50 % of the initial capital expenditure [1] and represents the greatest potential for LCOE reduction among capital equipment costs [2].

Heliostat costs are generally specified in $/m^2. This measure is, however, misleading because it does not take optical performance into account. Kolb *et al.* [1] show that smaller, more accurate heliostats with significantly higher cost, on a $/m^2 basis, result in the same LCOE due to a reduction in the tower height, receiver area and number of heliostats required. A $/m^2 value is does thus not necessarily relate to LCOE.

The principal purpose of a heliostat is to reflect the solar irradiance onto the receiver aperture. The flux density distribution of the reflected radiation on the receiver aperture can be mathematically characterised as aN angular standard deviation from the central ray [3]. This deviation is referred to as the total beam dispersion error and is represented by σ_{Tot}. If the σ_{Tot} term can be reduced in such a way that the optical advantages achieved outweigh the accompanying $/m^2 cost increase, a reduction in the LCOE can be achieved.

Assuming statistical independence, σ_{Tot} can be written as a function of its constituents:

$$\sigma_{Tot}^2=\sigma_{sun}^2+\sigma_{BQ}^2+\sigma_{astig}^2 \quad (1)$$

σ_{sun} is representative of the sunshape. The solar cone angle is approximated to 2.3 mrad but can reach much higher values depending on atmospheric conditions [4].

σ_{BQ} describes the beam quality of the heliostat. The beam quality is the term for the contributions of the optical errors of the heliostat such as: surface slope errors, tracking inaccuracies as well as wind, gravity and thermal loading. Kolb *et al.* [1] also show that these factors correlate with the \$/m\s^2 cost of a heliostat.

σ_{astig} accounts for astigmatic aberration of the reflective surface profile. This term is dependent on the canting strategy and the facet profiles chosen, as well as the slant range, focal ratio, incidence angle and the alignment angle at any instant in time. The annual variation of this term is thus unique to each heliostat, its tracking mechanism and location.

Canting is the optical alignment of facets of a heliostat on the common support structure and is used to collectively focus the individual facets. Canting strategies are known to have a major influence on field performance. Selecting an appropriate canting strategy will allow σ_{astig} to be reduced, resulting in an annual improvement of the total beam dispersion error, σ_{Tot}. The fact that heliostat facets require precision alignment regardless of the canting strategy suggests that the choice of canting strategy may not necessarily have cost implications [5]. Selecting the optimum canting strategy may therefore result in reductions of the LCOE.

The four prevalent canting strategies are on-axis (ON), off-axis (OFF), parabolic (PAR) and target aligned (TA) canting as defined below:

ON - facets are aligned to produce the minimum image area when the sun, target and heliostat are collinear (spherical profile).

OFF - facets are aligned to produce the minimum image area for a specific sun position, specified by canting time and date (toroidal profile).

PAR - facets are aligned to form a paraboloid stretched in the x and y axis (toroidal profile).

TA - facets are aligned to produce the minimum image area for a specific sun position on a target aligned tracking heliostat, specified by canting time and date (toroidal profile).

Buck and Teufel [5] compared and optimised these four canting mechanisms numerically using the Monte Carlo based MIRVAL ray-tracer. The simulations were computationally expensive and required ten million rays per simulation. This study aims to assess the viability of determining the performance of canting strategies analytically with the HFLCAL modelling tool.

2. The HFLCAL model

The HFLCAL model is a mathematical model to determine the flux density distribution. The model was developed for two reasons; firstly to determine in a computationally inexpensive manner the annual plant output for a given field configuration and secondly, to ascertain the field layout and total system optimisation with respect to the maximum annual electric energy yield per collector unit [6]. Although the model has been further developed to include additional features [6], the interest for this paper lies in the modelling of the flux density distribution. HFLCAL was specifically selected due to the simplicity in which canting can be incorporated. Validation cases of the model can be found in [7].

2.1. HFLCAL outline

Although some relevant aspects of the model are discussed here, the reader is referred to [6] and [7] for further detail.

The model approximates the flux density distribution of a single heliostat statistically as a circular normal distribution.

$$\text{Flux}(x,y) = \frac{P_h}{2\pi\sigma_i^2}\exp\left(-\frac{x^2+y^2}{2\sigma_i^2}\right) \tag{2}$$

The distribution is dependent on the beam power, P_h, and the radial standard deviation of the image, σ_i. σ_i is simply calculated from the product of beam dispersion error, σ_{Tot}, and the slant range, d. The incidence angle on the receiver, φ_{rec}, is taken into account here by dividing by the square root of its cosine.

$$\sigma_i = \frac{d\,\sigma_{Tot}}{\sqrt{\cos(\varphi_{rec})}} \tag{3}$$

2.2. Incorporating canting into HFLCAL

The canting strategy influences the σ_{astig} (see Equation 1) which is determined from the astigmatism of the image. Assuming an elliptical image, Guo and Wang [8] compare methods to fit elliptical Gaussian function to circular Gaussian functions. To determine the radial power distribution the square mean average of the standard deviations in the major and minor axes is most appropriate (Equation 4). It should be noted that when investigating peaks in the flux distribution the geometric mean (Equation 5) should rather be used [8].

$$\sigma_{astig}^2 = \frac{(\sigma_{major}^2+\sigma_{minor}^2)}{2} \tag{4}$$

$$\sigma_{astig}^2 = \sigma_{major}\sigma_{minor} \tag{5}$$

Igel and Hughes [9] use the curvature in the tangential and sagittal planes at the edges of a circular heliostat to calculate σ_{major} and σ_{minor}. This technique is adopted here and canting strategies are incorporated by determining the resulting edge curvatures in the tangential and sagittal planes.

Previous literature on canting strategies consider the Annual Incident Power Weighted Intercept (AIPWI) to be the most appropriate figure of merit with which to evaluate canting strategies [5, 10]. The AIPWI is defined as the fraction of absorbed irradiation that arrives at the receiver annually and is a percentage measure of annual spillage losses. The AIPWI considers only intercept effects, and although a high AIPWI is a requirement for efficient heliostat performance, other effects such as cosine losses can result in a heliostat with a high AIPWI to perform poorly [5]. The intercept efficiency at any point in time can be determined by integrating the flux density distribution over the receiver area. The AIPWI is the annual sum of the integrals divided by the total annual beam power (Equation 6).

$$\text{AIPWI} = \frac{\sum \frac{P_h}{2\pi\sigma_r^2}\left(1-\exp\left(-\frac{r^2}{2\sigma_r^2}\right)\right)}{\sum P_h} \tag{6}$$

2.3. Error correction for high receiver incidence angles

During the validation process it was observed that the AIPWI was underestimated at high receiver incidence angles, φ_{rec}, and low total beam dispersion errors, σ_{Tot}, relative to ray traced solutions (Figure 1). The radial power distribution function obtained by the HFLCAL at varying φ_{rec} and σ_{Tot} was compared to a numerical integration of the flux distribution function. The numerical solution was integrated over an elliptical area, corresponding to the cosine projection of a circular receiver aperture.

It was found that by adjusting for receiver incidence with $\sqrt{\cos(\varphi_{rec})}$ (Equation 3) underestimated intercept efficiencies at both high φ_{rec} and low σ_{Tot}. A surface fit was done on the numerical integrals to find a minimised error function for a φ_{rec} range of 20° to 70° and σ_{Tot} range of 0.5 mrad to 3 mrad. Intercept errors resulting from the high φ_{rec} were reduced to 0.5 % in the range by replacing the term $(\cos(\varphi_{rec}))^{0.5}$ in Equation

3 by $(\cos(\varphi_{rec}))^{0.3044}$. A corrective for φ_{rec} was not attempted.

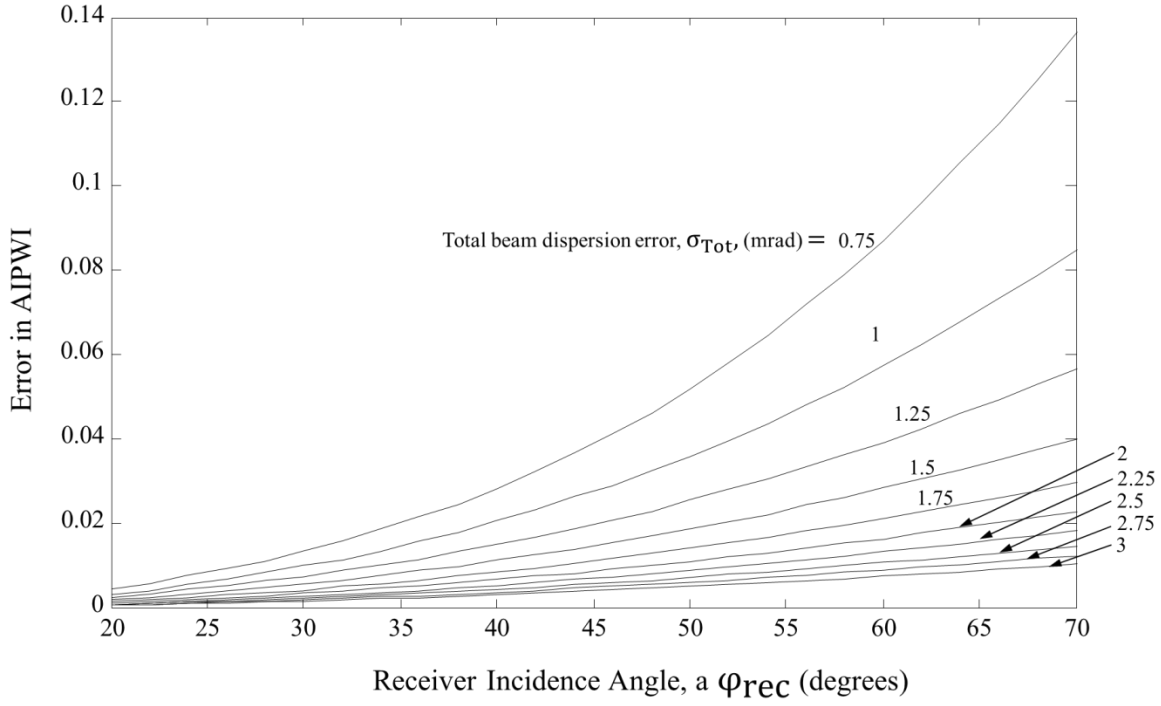

Fig. 1. The Annual Incident Power Weighted Intercept underestimation of the HFLCAL method relative to a numerical integration technique

3. Case study

To assess the validity of the HFLCAL model a case study was required where the performance of canting strategies are known. To the knowledge of the author, the only publicly available study of this kind is that of Buck and Teufel [5] and is thus used as a reference case in this paper. Buck and Teufel's study adopts the analysis of a $100kW_e$ minitower system with a 1.02 m diameter circular receiver aperture tilted 43° downward and utilises a field of 16 m^2 heliostats. This study considers only on-axis and off-axis canting utilising only Azimuth-Zenith tracking.

One discrepancy between the case study and the model is that HFLCAL cannot assess rectangular heliostat apertures. To account for this, the spillage losses from the corners of the heliostat was assumed to be represented by a $1-\pi/4$ factor (ratio of the area of a circle to the area of a square of the same chord length) and added to the AIPWI results from the Buck and Teufel study. At low slant range the corner areas are less susceptible to intercept losses which accounts for the high AIPWI values reported by Buck and Teufel for low tower multiples (see Section 3.1) in Figure 2. Further implications of this assumption are unknown.

3.1. On-axis canting

On-axis canting is the simplest strategy and facets are canted to form a spherical shape with a radius of 2d. The AIPWIs of individual on-axis canted heliostats were compared for three radial fans in the field (Figure 2). The heliostats position was specified by its radial distance from the tower base, normalised as a multiple of the tower height, R, and position angle, θ ($\theta_0 \rightarrow$E and $\theta+ \rightarrow$N).

The results show that as heliostats move further away from the tower the AIPWI decreases. This is expected due to the image size being a function of the slant range. Secondly a decrease in the AIPWI is observed for

the angular position in the field. This is also expected due to increases in φ_{rec}. The 90° radial fan performs best since the receiver aperture faces north. As the heliostat position moves eastward φ_{rec} increases resulting in a drop in the AIPWI, as observed in for 60° and 30° fans.

HFLCAL overestimated the AIPWI by 1 % to 5 % for large portions of the field. The largest discrepancy is observed near the base of the tower where the model starts to underestimate the AIPWI. This is consistent with the earlier finding that at low σ_{Tot}, intercept errors are underestimated (Section 2.3). The significant result is that the data trend for both a 30° and 90° radial fans replicate the trend consistently. Only 30° and 90° radial fan data are available from are available from [5].

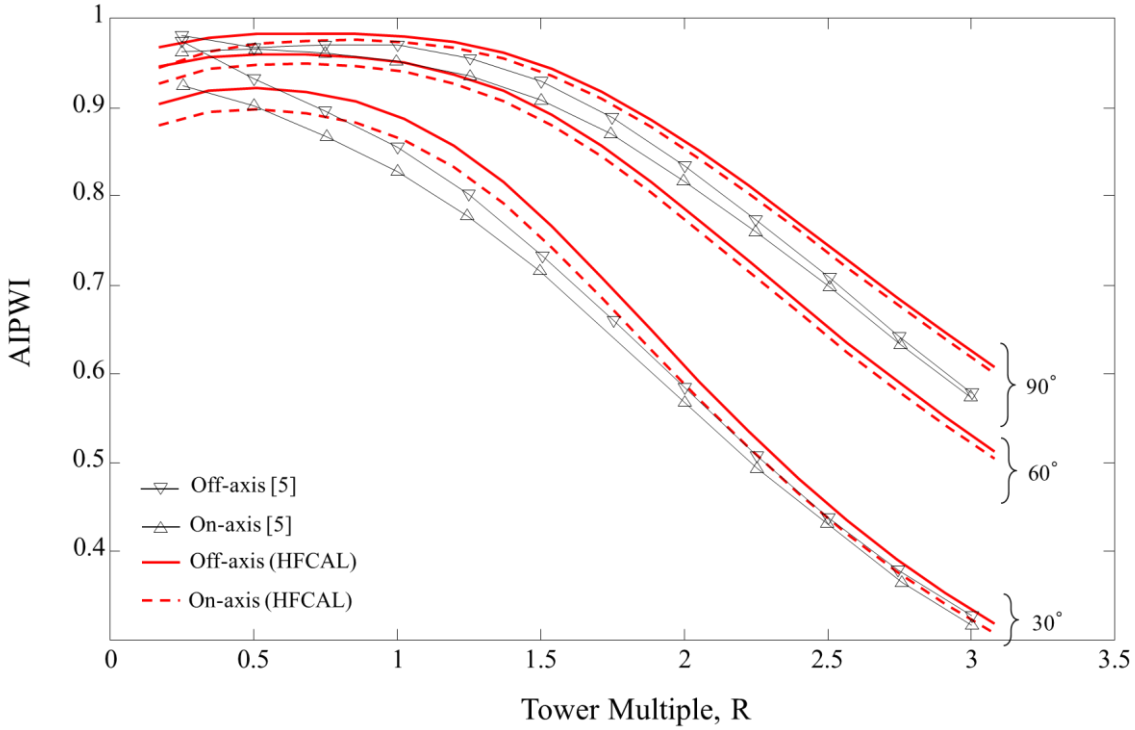

Fig. 2. The Annual Incident Power Weighted Intercept of on-axis and off-axis canting strategies, for 30°, 60° and 90° radial fans, at varying radial tower multiples from the tower base

3.2 Off-axis canting

Comparing off-axis tracking is more complex since two orthogonal radii of curvature must be specified at an optical alignment angle. The radii of curvature and optical alignment angle are related to time. The values of these parameters can be set to produce an aberration free image at a specified date and time. The AIPWI at various off-axis canting times was compared to that of Buck and Teufel for 30° and 90° radial fans, as shown in Figure 3

The HFLCAL model replicates optimum canting times at 9h30 near day 175 or 14h00 near day 300. Some discrepancy was observed and the AIPWI is overestimated for mid-day canting in summer (northern hemisphere).

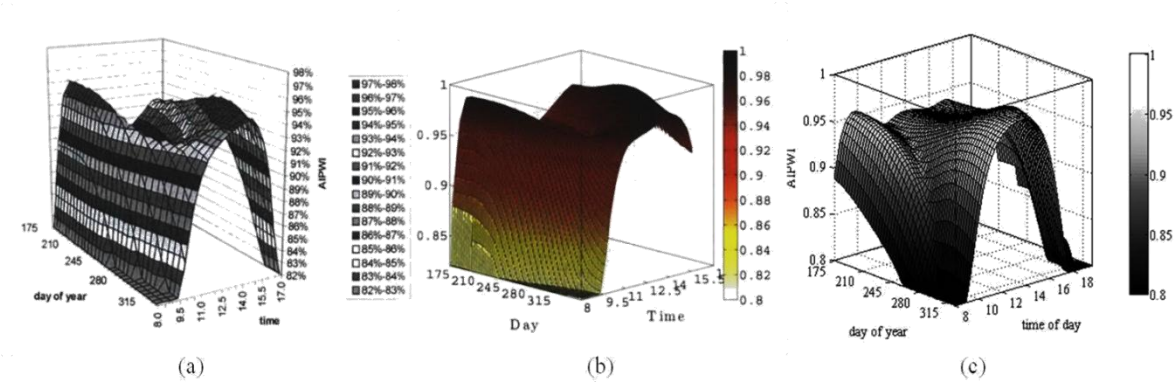

Fig. 3. Annual Incident Power Weighted Intercept for various off-axis canting dates and times (a) Buck and Teufel [5] (b) Noone [11] (c) HFLCAL

Optimum off-axis canting for the 30° and 90° radial fans are compared to on-axis canting in Figure 2. Again the results replicate the trend. Off-axis canting achieved higher AIPWI than on-axis canting by between 1 % and 3 %.

If canting strategies are to be optimised, the relative performance between strategies is most important. The relative performance shows good correlation and indicates that HFLCAL is suitable to compare canting strategies. The data discrepancies, however, suggest that this analytical approach is not suitable for detailed design.

4. Conclusions

The HFLCAL model was found to underestimate the image intercept with increasing receiver incidence angles and low beam dispersion errors. Adapting the way in which HFLCAL deals with the receiver incidence allowed for improvement in the model accuracy.

The limitations of circular heliostat apertures can be addressed by adjusting the AIPWI by a $1-\pi/4$ factor, however, the implications of this assumption are unknown and should be investigated in a future study.

The AIPWI is dependent on field position and decreases with increasing φ_{rec} and d. The AIPWI also varied according to the canting strategy and for this case study off-axis canting outperforms on-axis canting by between 1 % and 3 %.

The model was able to replicate trends in the AIPWI variation for both on and off-axis canting strategies at varied positions of the field and generally overestimated AIPWI by less than 5 %. It is concluded that the model is appropriate for preliminary analysis of canting strategies and provides an analytical tool that is computationally inexpensive.

Acknowledgements

The authors acknowledge with thanks the support for this work by the STERG that made funds available through the Solar Spoke of the DST, the NRF and the Stellenbosch University Hope Project.

References

[1] G. J. Kolb, S. A. Jones, M. W. Donnelly, D. Gorman, R. Thomas, R. Davenport, R. Lumia, Heliostat cost reduction study, Tech. rep., SAND-2007-3293, Sandia National Laboratories, Albuquerque, NM (2007).

[2] G. J. Kolb, C. K. Ho, T. R. Mancini, J. A. Gary, Power tower technology roadmap and cost reduction plan, Tech. Rep. Albuquerque, SAND-2011-2419, Sandia National Laboratories, Albuquerque, NM (2011).

[3] R. Monterreal, P. Heller, Large area heliostat comparison at PSA, Tech. rep., Plataforma Solar de Almería, Spain (1997).

[4] F. Biggs, C. N. Vittitoe, HELIOS model for the optical behavior of reflecting solar concentrators, Tech. rep., SAND-76-0347, Sandia National Laboratories, Albuquerque, NM (1979).

[5] R. Buck, E. Teufel, Comparison and optimization of heliostat canting methods, Journal of Solar Energy 131 (2009) 11001–11008.

[6] P. Schwarzbözl, M. Schmitz, R. Pitz-Paal, Visual HFCAL - a software for layout and optimization of heliostat fields, in: Proceedings of the SolarPACES Conference, Berlin, Germany, 2009.

[7] F. J. Collado, One-point fitting of the flux density produced by a heliostat, Solar Energy 84 (2010) 673–684.

[8] M. Guo, Z. Wang, On the analysis of an elliptical Gaussian flux image and its equivalent circular Gaussian flux images, Solar Energy 85 (2011) 1144–1163.

[9] E. A. Igel, R. L. Hughes, Optical analysis of solar facility heliostat, Solar Energy 22 (1979) 283–295.

[10] S. A. Jones, A comparison of on-axis and off-axis heliostat alignment strategies, Tech. rep., SAND-96-0566C, Sandia National Laboratories, Albuquerque, NM (1996).

[11] C. J. Noone, Optimization of central receiver concentrated solar thermal: site selection, heliostat layout & canting, Master's thesis, Massachusetts Institute of Technology, Cambridge, MA (2011).